Contrib Mineral Petrol (2006) 152:187–200
DOI 10.1007/s00410-006-0100-9

ORIGINAL PAPER

Platinum-group element, Gold, Silver and Base Metal distribution in compositionally zoned sulfide droplets from the Medvezky Creek Mine, Noril'sk, Russia

Sarah-Jane Barnes · R. A. Cox · M. L. Zientek

Received: 3 October 2005 / Accepted: 25 March 2006 / Published online: 31 May 2006

Abstract Concentrations of Ag, Au, Cd, Co, Re, Zn and Platinum-group elements (PGE) have been determined in sulfide minerals from zoned sulfide droplets of the Noril'sk 1 Medvezky Creek Mine. The aims of the study were; to establish whether these elements are located in the major sulfide minerals (pentlandite, pyrrhotite, chalcopyrite and cubanite), to establish whether the elements show a preference for a particular sulfide mineral and to investigate the model, which suggests that the zonation in the droplets is caused by the crystal fractionation of monosulfide solid solution (mss). Nickel, Cu, Ag, Re, Os, Ir, Ru, Rh and Pd, were found to be largely located in the major sulfide minerals. In contrast, less than 25% of the Au, Cd, Pt and Zn in the rock was found to be present in these sulfides. Osmium, Ir, Ru, Rh and Re were found to be concentrated in pyrrhotite and pentlandite. Palladium and Co was found to be concentrated in pentlandite. Silver, Cd and Zn concentrations are highest in chalcopyrite and cubanite. Gold and platinum showed no preference for any of the major sulfide minerals. The enrichment of Os, Ir, Ru, Rh and Re in pyrrhotite and pentlandite (exsolution products of mss) and the low levels of these elements in the cubanite and chalcopyrite (exsolution products of intermediate solid solution, iss) support the mss crystal fractionation model, because Os, Ir, Ru, Rh and Re are compatible with mss. The enrichment of Ag, Cd and Zn in chalcopyrite and cubanite also supports the mss fractionation model these minerals are derived from the fractionated liquid and these elements are incompatible with mss and thus should be enriched in the fractionated liquid. Gold and Pt do not partition into either iss or mss and become sufficiently enriched in the final fractionated liquid to crystallize among the iss and mss grains as tellurides, bismithides and alloys. During pentlandite exsolution Pd appears to have diffused from the Cu-rich portion of the droplet into pentlandite.

Communicated by T. L. Grove

S.-J. Barnes (✉) · R. A. Cox
Sciences de la Terre, Université du Québec à Chicoutimi,
Quebec, QC, Canada G7H 2B1
e-mail: sjbarnesl@uqac.ca

M. L. Zientek
U.S. Geological Survey, Spokane Office,
Washington, WA 99201, USA
e-mail: mzientek@usgs.gov

Introduction

The concentration of platinum-group elements (PGE) and Au in sulfide minerals and their preference for a particular sulfide mineral is of interest for a number of reasons. Firstly, many models of how these elements behave during partial melting of the mantle assume that the PGE are mainly located in sulfides and are fractionated by partial melting of these sulfides (Brockrath et al. 2004; Griffin et al. 2002; Lorand and Alard 2002; Peregoedova et al. 2004). Secondly, the efficient extraction of PGE and Au known to be present in many Ni–sulfide ore-deposits requires a good understanding of the mineralogical sites of these elements in the ore. Thirdly, many Ni–sulfide ore deposits show compositional zonation with respect to Cu, Fe, PGE and Au. For example the Oktyabr'sky massive sulfide deposit of the Noril'sk-Talnakh region

in Russia is mineralogically and compositionally zoned from a Cu–Pd–Pt–Au-rich center, dominated by Cu–Fe sulfides such as chalcopyrite and mooihoekite, to Fe–Os–Ir–Ru–Rh-rich margins composed primarily of pyrrhotite (Czamanske et al. 1992; Distler 1994; Stekhin 1994). The origin of the compositional zonation is thought to be fractional crystallization of an Fe–Ni–Cu sulfide liquid, with the Fe-rich portions representing the monosulfide solid solution (mss) cumulate and the Cu-rich portions representing the fractionated liquid, which crystallizes as intermediate solid solution (iss) (Distler 1994; Naldrett et al. 1994; Zientek et al. 1994).

Experimental work has shown that the partitioning behavior of most of the chalcophile elements into mss is negatively dependent on the metal/S ratio or $f\,S_2$ of the sulfide system (Li et al. 1996; Barnes et al. 2001; Ballhaus 2001; Sinyakova et al. 2001; Mungall et al. 2005). In a basaltic melt the metal/S ratio of an immiscible sulfide is controlled in turn by the $f\,O_2$, which should be close to FQM and thus $f\,S_2$ should be in the range –2 to 0 (Wallace and Carmichael 1992). At these $f\,S_2$ Os, Ir, Ru Rh and Re partition into mss, while Pt, Pd, Au and Ag concentrate in the Cu-rich sulfide liquid (Table 1). At high temperatures the partition coefficient for Ni into mss a, is slightly below 1, but as the temperature falls Ni becomes slightly compatible with mss (Li et al. 1996; Barnes et al. 2001). Cobalt shows behavior intermediate between Ni and Cu (L.A. Rose Unpublished thesis). Empirical observation suggests that Cd and Zn concentrate in the liquid (e.g., Zientek et al. 1994). As the temperature falls the mss exsolves into pyrrhotite and pentlandite and iss exsolves into chalcopyrite ± cubanite plus pentlandite. During, exsolution PGE and other metals that originally partitioned into mss and iss could migrate to grain boundaries and form platinum-group minerals (Makovicky et al. 1986; Makovicky 2002), or they could partition into the newly formed pyrrhotite, pentlandite, chalcopyrite and cubaniteminerals.

Sulfide droplets 1–3 cm in size are found in some of the subvolcanic intrusions of the Noril'sk area. The upper parts of the droplets are enriched in Cu-rich sulfides and the base is rich in pyrrhotite. By analogy with the large zoned massive sulfide bodies such as Oktyabr'sky this type of droplet has been interpreted as to be the product of crystal fractionation of a sulfide liquid (Czamanske et al. 1992; Lightfoot et al. 1984; Prichard et al. 2004). These droplets represent an ideal opportunity to investigate the behavior of PGE during the crystallization of a sulfide liquid because the rocks have not been metamorphosed since they were emplaced and the system is relatively closed. We have determined the PGE, Au, Ag, Cd, Co, Re and Zn concentrations in the sulfide minerals to investigate: (a) whether sulfide minerals are the principal host of these elements, (b) whether the metals partition preferentially into a particular sulfide mineral, (c) whether mss fractionation could explain the zonation observed in the droplets.

Petrographic observations

The mineralogy of the Noril'sk ores has been described in detail by many authors (e.g., Genkin et al. 1982; Distler 1994) and it is not the purpose of this paper to duplicate previous work on the mineralogy of Noril'sk sulfides. However, some petrographic observations concerning our samples are relevant in interpreting the analytical results. Our samples are from the Medvezky Creek Mine of Noril'sk I intrusion. Polished sections of three droplets and one Cu-rich massive sulfide vein were examined with a petrographic microscope and sites were selected for microbeam analysis of two droplets from sample AB, one droplet from sample from E-1 and massive sulfide A-2. The major element compositions of the sulfides were determined by energy dispersive X-ray analysis

Table 1 Partition coefficients for the metals between monosulfide solid solution and base metal sulfide liquid in alloy free systems (900–1,200°C)

Ni	Cu	Co	Os	Ir	Ru	Rh	Pt	Pd	Au	Ag	Re	References
0.84	0.27		4.3	3.6	4.2	3.03	0.2	0.2	0.09			Fleet et al. (1993)
0.3–2	0.2–0.25			3.4–17		1.16–5.6	0.05–0.23	0.08–0.24				Li et al. (1996); Barnes et al. (2001)
0.5–0.9	0.2–0.3		4–7		5–10					0.5		Peregoedova et al. (2006)
0.6–1.1	0.19–0.29		5	3.1–11.8	3–19	1.5–3.5	0.017–0.13	0.058–0.19				Ballhaus et al. (2001)
0.54–0.74	0.26–0.28		3.8								2.5	Brenan et al. (2002)
0.8	0.2			7.37	14.25	5.6	0.04	0.08	0.01			Mungall et al. (2005) QFM-2
0.59–0.91				> > 1	> > 1	3.5–8.3	0.02–0.06	0.04–0.08				Sinyakova et al. (2001)
		0.313–0.512										Rose (1998)

using the microprobe at the University of Laval (Table 2).

The sulfide droplets are found in a varitextured gabbronorite (the local term for this is a taxitic gabbro). The droplets are 1–3 cm in size (Fig. 1a) with the upper two thirds of each droplet consisting of an intergrowth of cubanite and chalcopyrite with elongate exsolutions of pyrrhotite (0.02×0.1 mm) (Fig. 1b). The lower portion of the droplets consists of pyrrhotite with very small (0.05×0.01–0.01×0.003 mm) flame exsolutions of pentlandite (Fig. 1c). Between the pyrrhotite and Cu–sulfide is a layer of granular pentlandite (Fig. 1a). The pentlandite contains fractures (0.01–0.05 mm wide) filled with magnetite. The pentlandite also contains patches of exsolved pyrrhotite (0.02–0.05 mm in diameter). Euhedral ilmenite crystals approximately 1 mm in length are present at the margins of some of the droplets.

The massive sulfide Cu-rich vein consists predominantly (~75 modal percent) chalcopyrite, which contains large (1–2 cm) crystals of subhedral pentlandite (~25 modal percent).

Method

The PGE, Ag, Au, Cd, Co, Re and Zn concentrations were determined by laser ablation induced coupled plasma mass spectrometry (LA-ICP-MS) at the University of Quebec, Chicoutimi (UQAC). The method used follows that of Cox and Barnes (2005) and is described briefly here. The laser employed was a New Wave Research Nd: YAG UV laser operating at 213 nm. The beam size was 80 μm, with a power of 0.8 mj/pulse for Globules AB-1 and AB-2. A beam size of 40 μmwith a power of 0.25 mj/pulse was used for Globule E-1 and massive sulfide A-2. Laser frequency was maintained at 20 Hz for all analyses, which resulted in cylindrical laser pits of 40–100 μm deep (see Fig. 1). Ablation was carried out using a helium carrier gas, which continually flushed the airtight laser cell, and was mixed with argon before entering the ICP-MS. The ablated material was analyzed using a Thermo X7 quadrupol ICP-MS operating in time resolved mode using peak jumping using a dwell time of 10 m sec/peak. The transition metals Fe, Co, Ni, Cu were measured in a high-resolution mode with a peak width of < 0.4 amu. All other elements were measured in standard resolution mode with a peak width of ~ 0.70 amu. The use of collision cell technology has been shown to greatly reduce argide interferences on the PGE's (Mason and Kraan 2002). The instrument was operated using a collision cell gas of mix of 7% H_2 in He with a flow rate of ~ 6 to 8 ml/min and tuned to minimize Ni, Cu and Zn argide signals.

The only reference material for determining PGE in situ in sulfides is a synthetic NiS bead (PGE-A) dopped with ~ 200 ppm of each PGE (Gemoc 2006). We have not used PGE-A in calibrating our machine for the following reasons: there is very little of this standard left, making it impractical to use it on a daily basis; also it contains an order of magnitude more PGE than most natural minerals, and thus does not necessarily provide an accurate estimation of the precision in natural minerals, and finally Ni produces various interferences on light PGE which can be corrected for, but there will always be some error in the correction and the error will be propagated through-out the analyses of the unknowns. Therefore, in order to calibrate we used a synthetic FeS (po52) doped with 5–10 ppm PGE and Au, prepared by Dr. Peregoedova at McGill University. Two batches of FeS were prepared, one PGE free and one containing 0.1 wt% PGE. Both the PGE-free and PGE-bearing FeS was prepared by weighing out reagent grade metals and S in the desired proportions. These were then mixed and placed in silica glass tubes and heated to 500°C over 7 days. The tubes were then heated in a vertical furnace at 1,260°C for 1 h to assure complete mixing of the elements. The temperature was then reduced in to 1,000°C at the rate of 1°C per minute. The charges were annealed at 1,000°C for 4 days. They were then quenched by dropping the tubes into cold salt water. In order to obtain FeS with only 1–5 ppm PGE the FeS with 0.1 wt% PGE was diluted with the PGE-free FeS. This was then heated for 1 h at 1,260°C and quenched in salt water. Pieces of the mixed FeS were then mounted and polished and examined by optical and electron microscopes for exsolutions of platinum-group minerals (PGM). No exsolutions were observed either optically or by back-scatter electron imagining. The FeS content of po52 was determined by microprobe analysis at McGill University as 61.05 wt% Fe and 38.62 wt% S.

Table 2 Major element concentrations in the sulfide minerals

Droplet	Mineral	*n*	S (wt%)	Fe (wt%)	Cu (wt%)	Ni (wt%)	Total (wt%)
AB-1	Cubanite	3	35.18	40.95	23.64	< 0.1	99.76
AB-1	Pyrrhotite	3	39.00	58.64	< 0.1	0.20	97.84
AB-1	Pentlandite	3	32.37	36.95	0.00	30.45	99.76
AB-2	Pentlandite	3	34.19	36.06	< 0.1	31.57	101.82
AB-2	Pyrrhotite	3	39.31	59.50	< 0.1	0.90	99.71
AB-2	Cubanite	2	35.23	41.40	21.45	< 0.1	98.08
AB-2	Chalcopyrite	2	34.28	31.88	32.83	< 0.1	98.99

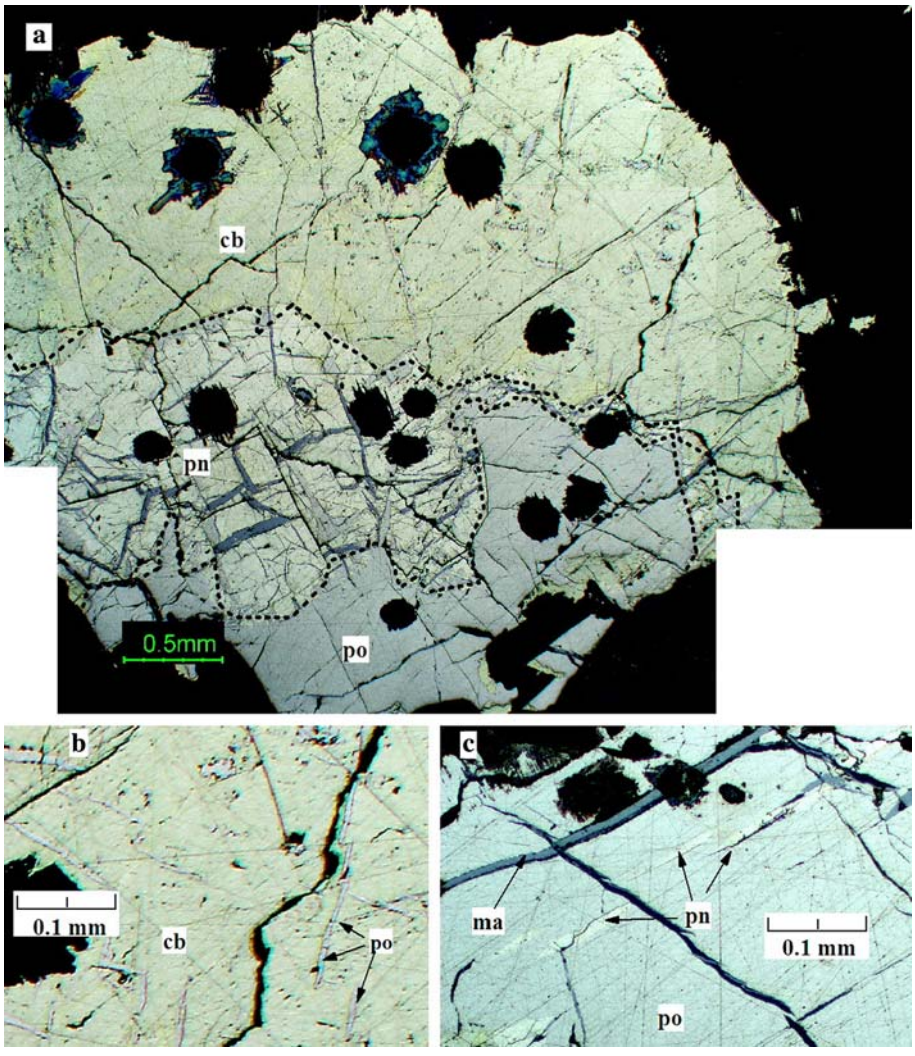

Fig. 1 Photomicrographs of sulfide droplets AB-1 and AB-2: **a** whole droplet (*AB-1*); showing cubanite-chalcopyrite intergrowth (*cb*) in the upper portion, pyrrhotite (*po*) in the lower portion, granular pentlandite between the upper and lower portions (*pn*); **b** exsolutions of pyrrhotite in cubanite–chalcopyrite intergrowth (*AB-2*); **c** pyrrhotite from lower portion of AB-2 with exsolutions of flame pentlandite and magnetite (*ma*) in fractures

The PGE and Au concentrations in po52 were determined by isotope dilution ICP-MS and wet chemistry by Dr Meisel at the University of Leoben using the method of Meisel et al. (2003) on 3 small ~10 mg aliquots (Tables 3, 4). These values were then used when calibrating the LA-ICP-MS with po52. The homogeneity of po52 was tested by determining the PGE contents by LA-ICP-MS in 16 different spots. The coefficient of variation is between 5 and 13% (Tables 3, 4). As a test of accuracy PGE and Au contents in the reference material PGE-A were determined and our results agree with recommended results within analytical error (Tables 3, 4). The concentrations of Cd, Co and Zn in po52 were determined by standard addition and ICP-MS at UQAC and then po52 was used for LA-ICP-MS calibration (Table 5). The coefficient of variation for these elements is 8–15%. A NiS fire assay bead similar to PGE-A was doped with ~ 2 ppm Ag and Re, the exact concentrations were determined by standard addition and ICP-MS at UQAC (Table 5). This bead was then used for calibration during LA-ICP-MS. The coefficient of variation on four determinations was 6–8%. As a final indication of the accuracy of the results we would point out that some elements have been determined in Noril'sk sulfides by other workers and our results are broadly in agreement with the previous studies, thus we feel the results are accurate.

The detection limits as defined by three sigma times the background is in the 0.0001–0.008 ppm range for FeS (Tables 3, 4). In order to test the efficiency of the collision cell and to more closely approximate the matrix effects of natural Ni and Cu sulfides, a NiS_2 and $CuFeS_2$ blank were synthesized in the same manner as po52. Based on the counting statistics of these blanks the detection limits in pentlandite, chalcopyrite and cubanite are 5–10 times higher than in FeS (Tables 3, 4). All data were reduced using PlasmaLab software, with ^{34}S as the internal standard, and follows the general method Jackson et al. (1992).

Table 3 Estimation of accuracy and precision for PGE and Au for LA-ICP-MS analyses

Sample	Method; laboratory	*n*	101Ru (ppm)	103Rh (ppm)	105 Pd (ppm)	108Pd (ppm)	192Os (ppm)	193Ir (ppm)	195Pt (ppm)	197Au (ppm)
PO-52	Solution, Leoben[a]	3	5.30	6.58	8.67	8.67	11.60	4.33	9.01	11.28
	± 1 sigma		0.25	0.50	0.65	0.65	1.20	0.20	0.65	
PO-52	LA-ICP-MS, UQAC	16	5.32	6.61	8.61	8.66	11.68	4.37	9.04	11.27
	± 1 sigma		0.32	0.53	0.80	0.81	1.70	0.61	1.27	1.44
PGE-A	LA-ICP-MS, UQAC	6	214	198	298	262	191	164	153	290
	± 1 sigma		12	12	20	16	16	12	10	20
PGE-A	PIXE, Gemoc[b]	4	226	235	310	310	180	103	122	234
	± 1 sigma		26	31	68	68	96	52	16	13
PGE-A	LA-ICP-MS, Gemoc[b]	172	205	223	274	274	199	211	124	212
	± 1 sigma		11	12	13	13	9	12	7	11

[a]Isotope dilution analysis and wet chemical analysis (Meisel 2003)

[b]Gemoc (2006)

+ Detection limit = 3 × square root of the back ground counts, sigma = 1 standard deviation for *n* in different spots

Table 4 Estimation of + detection limits for PGE and Au by LA-ICP-MS analyses, for various matrixes

FeS PO-52	Average	8	0.0038	0.0015	0.011	0.0044	0.0008	0.00048	0.0007	0.00038
	± 1 sigma		0.0006	0.0002	0.002	0.0013	0.0002	0.000002	0.0005	0.00049
NiS_2 blank	Average	2	0.097	0.019	0.088	0.055	0.0016	0.0018	0.0033	0.0035
	± 1 sigma		0.095	0.016	0.025	0.062	0.0003	0.0002	0.0018	0.0001
$CuFeS_2$ blank	Average	2	0.140	0.019	0.11	0.042	0.011	0.0034	0.034	0.012
	± 1 sigma		0.400	0.049	0.04	0.064	0.007	0.0057	0.054	0.025

+ Detection limit = 3 × square root of the back ground counts, sigma = 1 standard deviation for *n* different spots

Fine scale (< 40 μm) exsolutions are common in sulfides. In order to properly assess the correlation between transition metal and trace-element concentrations, all the time resolved data were further screened for large-scale Ni and Cu fluctuations. The chalcopyrite and cubanite analyses are all from iss parts of the droplets, except for one analysis of the cubanite enclosed in the pentlandite between the iss and pyrrhotite. The pentlandite analyses are all of the granular pentlandite between the iss and pyrrhotite. The mss analyses also came from these areas. Pyrrhotite analyses are from the lower part of the droplets.

Table 5 Concentrations of trace elements in UQAC internal standards

	Method	*n*	Co (ppm)	Cd (ppm)	Zn (ppm)
PO-52	Standard addition	4	14.5	0.157	134
	± 1 sigma		1.2	0.023	9.4
			Ag (ppm)	Re (ppm)	
NiS-1.6	Standard addition	4	2.65	1.32	
	± 1 sigma		0.15	0.092	

Results

On the basis of the partition coefficients of the metals into mss (Table 1) and empirical observations from massive sulfides Cu, Ag, Au, Cd, Zn, Pt and Pd might be expected to concentrate in the fractionated liquid and thus could have concentrated in the iss that crystallized from the fractionated liquid and which is now represented by cubanite and chalcopyrite. In order to investigate this and to compare our results with those obtained by Czamankse et al. (1992) and Cabri et al. (2002, 2003) and to consider the mass balance, we have plotted our results for these elements (Table 6) versus Cu (Figs. 2a–d). Zinc, Cd and Ag do show a positive correlation with Cu, with each globule having a slightly different trend. The chalcopyrite and cubanite (triangles Fig. 2a) contain 200–1,200 ppm Zn (Tables 5, 6); these values are similar to those obtained by Czamanske et al. (1992) (open diamonds Fig. 2a). Pentlandite, mss and pyrrhotite contain considerably less Zn at 1–50 ppm (squares and circles Fig. 2a; Tables 5, 6). This is in agreement with Czamanske et al. (1992) who report that Zn concentrations for pentlandite and pyrrhotite are less than the Proton induced X-ray emission (PIXE) detection limit of approximately 50 ppm.

Table 6 Metal contents of sulfides from Noril'sk-1 as determined by LA-ICP-MS

Droplet	Mineral	61Ni (wt%)	65Cu (wt%)	59Co (ppm)	185Re (ppm)	192Os (ppm)	193Ir (ppm)	101Ru (ppm)	103Rh (ppm)	195Pt (ppm)	108Pd/ 105Pd[a] (ppm)	197Au (ppm)	107Ag (ppm)	111Cd (ppm)	67Zn (ppm)
AB-1	Cubanite	0.16	24.2	18	0.001	0.006	< 0.003	ND	0.379	0.581	9.2	0.069	51.0	3.80	611
AB-1	Cubanite	0.19	23.7	22	0.002	0.002	0.005	ND	0.448	0.822	10.1	0.071	51.9	4.20	705
AB-1	Cubanite	0.66	22.3	69	0.002	< 0.002	< 0.003	ND	0.386	0.453	19.5	0.064	45.9	2.97	531
AB-1	Cubanite	0.70	24.8	63	0.003	0.007	0.006	ND	0.454	0.793	20.6	0.078	44.7	2.78	437
AB-1	Cubanite	1.09	22.3	103	0.002	< 0.002	0.007	ND	0.400	1.17	21.8	0.040	47.4	2.58	447
AB-1	cb in pn	2.92	20.8	235	1.728	13.56	1.188	ND	0.629	10.93	69.2	0.662	55.0	3.35	646
AB-2	Cubanite	1.25	22.,4	191	0.005	0.068	0.014	ND	2.25	11.28	24.9	0.058	30.0	10.6	200
AB-2	Cubanite	2.48	22.9	194	0.006	0.026	< 0.003	ND	1.53	0.700	22.7	0.020	33.3	12.7	264
E-1	Cubanite	0.89	26.4	138	0.005	0.009	0.004	ND	2.12	1.49	7.98	< 0.016	ND	5.96	1276
E-1	Cubanite	2.81	24.0	481	0.009	0.093	0.187	ND	2.68	29.60	17.7	< 0.016	ND	5.10	565
E-1	Chalcopyrite	1.92	39.1	315	0.009	0.030	0.021	ND	2.98	9.12	14.2	< 0.016	ND	7.69	1318
E-1	Chalcopyrite	0.83	32.2	141	0.007	0.057	0.035	ND	2.79	17.97	6.73	< 0.016	ND	6.72	1280
AB-1	Pentlandite	32.1	0.168	2843	0.400	3.01	3.51	11.0	42.8	5.71	426	0.063	18.6	0.61	17.4
AB-1	Pentlandite	33.8	0.181	2694	0.339	3.09	3.73	11.6	74.6	5.09	527	0.614	18.4	0.55	8.9
AB-1	Pentlandite	35.3	0.094	2844	0.370	3.39	3.60	12.3	39.6	8.48	428	0.297	10.3	0.45	2.1
AB-2	Pentlandite	30.5	0.046	3309	0.171	1.37	1.55	10.2	40.8	19.0	600	3.26	16.2	2.35	3.3
AB-2	Pentlandite	34.0	0.126	4018	0.177	1.61	1.98	11.3	55.5	31.1	1052	2.03	32.4	2.29	2.9
AB-2	Pentlandite	35.6	0.223	4724	0.171	1.96	1.98	11.5	51.7	17.3	402	3.06	11.1	2.41	5.6
E-1	Pentlandite	29.0	0.006	4659	0.202	0.551	1.20	3.3	15.6	13.2	715	0.005	ND	2.37	11.6
E-1	Pentlandite	27.0	0.901	4389	0.250	0.649	1.42	3.5	18.1	7.91	842	0.007	ND	2.19	12.4
E-1	Pentlandite	26.9	4.299	4590	0.512	1.27	3.13	4.5	33.1	15.5	822	0.007	ND	2.69	30.2
E-1	Pentlandite	30.6	0.171	5426	0.186	0.491	1.04	3.4	12.2	12.6	446	0.009	ND	2.54	10.3
AB-1	Pyrrhotite	0.18	0.000	11	0.319	3.57	3.90	12.5	54.9	1.80	1.08	0.030	1.59	0.38	0.6
AB-1	Pyrrhotite	1.59	0.164	125	0.367	3.50	4.38	13.9	90.9	12.7	15.4	0.094	3.01	0.37	2.5
AB-2	Pyrrhotite	0.57	0.007	75	0.204	2.47	2.44	11.7	63.4	14.9	6.27	0.158	1.30	1.62	1.2
AB-2	Pyrrhotite	1.21	0.018	145	0.220	1.79	1.97	11.3	54.9	12.7	2.95	1.05	3.04	1.97	2.5
E-1	Pyrrhotite	0.59	0.008	103	0.168	0.427	0.98	2.5	16.5	20.2	3.01	0.101	ND	1.78	9.6
E-1	Pyrrhotite	0.85	0.012	163	0.178	0.505	1.00	2.6	16.8	27.2	2.29	0.169	ND	1.84	9.0
E-1	Pyrrhotite	0.42	0.005	51	0.208	0.464	1.09	2.4	16.2	13.3	1.79	0.035	ND	1.60	7.4
E-1	Pyrrhotite	0.34	0.005	37	0.203	0.520	1.15	2.4	13.9	19.4	1.96	0.024	ND	1.44	9.4
AB-1	MSS	6.9	0.911	588	0.399	3.27	3.88	12.4	73.0	9.14	70.1	0.071	6.88	0.39	18.8
AB-1	MSS	9.1	1.866	892	0.453	3.97	4.84	14.6	40.2	13.4	139	0.097	22.0	0.59	38.0
AB-1	MSS	9.3	0.010	891	0.405	3.65	4.51	14.0	73.0	5.26	97.7	0.062	10.0	0.56	1.0
AB-1	MSS	15.2	2.148	1851	0.525	4.37	4.91	14.8	63.1	9.21	271	0.104	40.4	0.67	53.9
AB-1	MSS	16.5	1.003	1477	0.433	3.33	4.07	11.6	47.1	9.03	205	0.054	22.0	0.55	38.3
AB-1	MSS	19.1	0.150	2209	0.286	2.81	3.83	11.6	76.3	11.9	234	0.075	12.2	0.38	8.1
AB-1	MSS	21.9	0.364	2439	0.367	3.66	4.27	13.9	70.6	5.4	223	0.088	23.7	0.99	27.0
AB-2	MSS	3.3	0.068	377	0.197	1.87	1.95	10.9	55.1	20.5	4.93	8.38	9.68	2.00	1.9
AB-2	MSS	11.9	0.670	1462	0.230	2.56	2.77	12.6	68.6	14.1	66.3	0.268	15.8	2.94	45.5

ND not determined

[a]In Cu-bearing sulfides 108Pd was used, in Ni and Fe-bearing sulfides 105Pd was used

Cadmium is concentrated in chalcopyrite and cubanite (3–12 ppm, Tables 5, 6; Fig. 2b) with pentlandite, mss and pyrrhotite containing considerably less (0.4–3 ppm). Czamanske et al. (1992) report similar Cd values for chalcopyrite and cubanite, but for pyrrhotite and pentlandite the PIXE detection limits were too high for them to obtain results.

The chalcopyrite and cubanite (triangles Fig. 2c) contain the most Ag (30–50 ppm, Tables 5, 6), the pentlandite contains slightly less (10–30 ppm, squares Fig. 2c) and the pyrrhotite the least (circles Fig. 2c) (1–30 ppm; Tables 5, 6). These results are similar to those obtained by Czamanske et al. (1992) (open diamonds).

Gold, Pt and Pd do not show positive correlations with Cu (Table 6). Neither do they correlate with one another. Platinum values cover a range between 0.3 and 30 ppm and Pt is not concentrated in any particular phase (Fig. 2d; Tables 5, 6). There are a few Pt results from Cabri et al. (2003) (diamonds on Fig. 2d), who report values slightly lower (0.02–2 ppm) than ours. The reason for the difference is not known.

Gold concentrations cover a similar range (0.03–10 ppm) to Pt and are extremely variable (Table 6). Furthermore, Au like Pt does not appear to be preferentially concentrated in a particular sulfide mineral (Tables 6, 7).

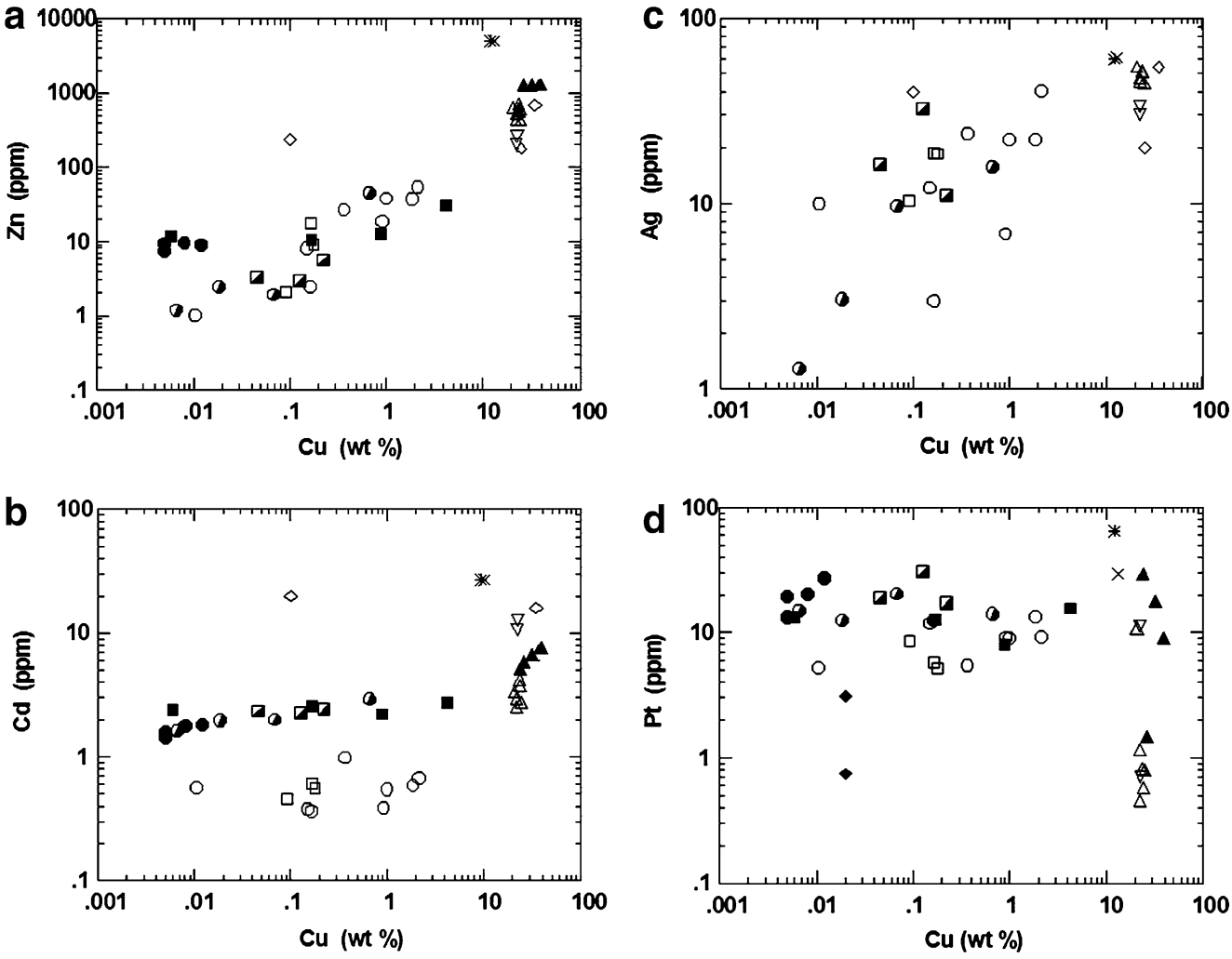

Fig. 2 Cu versus **a** Zn, **b** Cd, **c** Ag and **d** Pt. Note that the Cu-rich phases are enriched in Ag, Cd and Zn as is predicted by the mss fractionation model. In contrast Pt does not correlate with Cu despite the fact that Pt does not partition into mss. The sulfide liquid calculated from the whole rock composition (E-1 = * and AB = X) for Ag fall along the trend lines of the sulfides indicating Ag is largely present in sulfides. In contrast the amounts of, Cd, Pt and Zn calculated to be in the sulfide liquid lie above the trend lines indicating that these elements are present in other phases besides sulfides. *Circles* po, *triangles* cubanite or chalcopyrite, *squares* pentlandite, *open symbols* globule AB-1, *half filled symbols* droplet AB-2, *filled symbols* droplet E-1. *Diamonds* represent literature values; *open* Czamanske et al. (1992) and *filled* Cabri et al. (2002, 2003)

Palladium is strongly partitioned into pentlandite with values 200–1,200 ppm. Most chalcopyrite and cubanite contain 4–30 ppm Pd, although one cubanite grain found in the granular pentlandite has higher values (Table 6). Most pyrrhotite contains little Pd, with concentrations similar to cubanite at 1–10 ppm. However, some pyrrhotite appears to contain considerably more Pd at 100–200 ppm. This apparent anomaly can be resolved when we consider a plot of Ni versus Pd (Fig. 3a). There is a strong positive correlation between Ni and Pd and the pyrrhotite with high Pd concentrations also contains high Ni concentrations, which is probably due to the presence of small pentlandite exsolutions (Fig. 1c). Both Czamanske et al. (1992) and Cabri et al. (2003) obtained results for Pd and their values (diamonds) that were similar to ours.

Cobalt and Ni show a strong correlation (Fig. 3b) indicating that Co is concentrated in the pentlandite, with Co values in pentlandite between 0.2 and 0.6 weight percent. The data from Cabri et al. (2002) and Czamanske et al. (1992) fall on the same trend line as our data (Fig. 3b). However, data for Co in pyrrhotite reported in Czamanske et al. (1992) falls completely off this main trend and possibly the values for Co from the PIXE represent the detection limits.

The IPGE (Ir, Os, Ru and Rh) and Re all partition into mss (Table 1) and the mss crystal fractionation

Table 7 Average concentrations of the metals in the sulfide phases

Sample	Mineral	Ni (%)	Cu (%)	Co (ppm)	Re (ppm)	Os (ppm)	Ir (ppm)	Ru (ppm)	Rh (ppm)	Pt (ppm)	Pd (ppm)	Au (ppm)	Ag (ppm)	Cd (ppm)	Zn (ppm)
E-1	Droplet														
$n = 4$	cp/cb	1.61	30.44	269	0.008	0.047	0.062	ND	2.64	14.54	11.7	0.009	ND	6.37	1109
$n = 3$	Pentlandite	28.86	0.36	4825	0.213	0.564	1.216	3.37	15.27	11.24	667.6	0.007	ND	2.37	11.4
$N = 4$	Pyrrhotite	0.55	0.01	89	0.189	0.479	1.054	2.49	15.83	20.03	2.3	0.082	ND	1.66	8.9
AB	2 droplets														
$n = 7$	cp/cb	0.93	23.2	94	0.003	0.014	0.005	ND	0.84	2.26	18.4	0.057	43.47	5.66	456
$n = 6$	Pentlandite	33.54	0.14	3405	0.271	2.4	2.725	11.30	50.82	14.44	572.5	1.554	17.82	1.44	6.7
$n = 4$	Pyrrhotite	1.37	0.05	146	0.261	2.639	2.930	12.08	63.83	12.49	6.1	1.943	3.72	1.27	1.7
A-2	Massive sulfide														
$n = 4$	Cp	0.005	35.92	0.36	0.021	0.009	0.002	ND	3.18	0.10	5.15	0.006	ND	7.10	107
$n = 5$	Pentlandite	39.52	0.53	1627	0.036	0.128	0.006	1.81	2.55	7.66	1309	0.028	ND	1.88	<0.5

cp/cb chalcopyrite–cubanite intergrowth

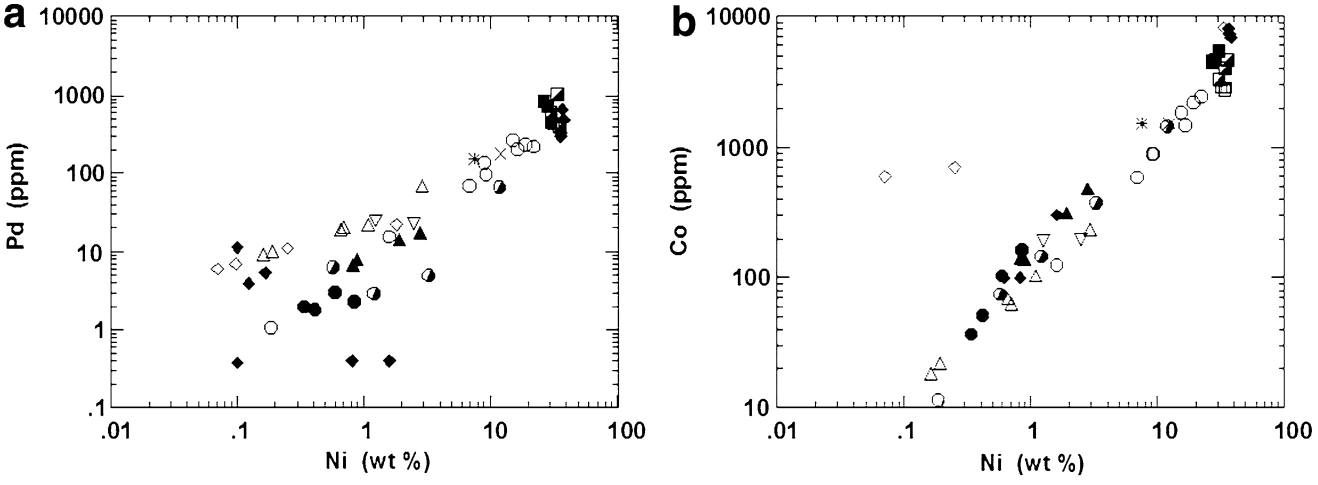

Fig. 3 Ni versus **a** Pd and **b** Co. See Fig. 2 for explanation of *symbols*. Note the strong correlation between Ni and these elements. The calculated sulfide-liquids (X and *) fall on the trend defined by the sulfide minerals suggesting that Ni and Co are largely contained in these sulfides

model predicts that they should correlate with each other. Iridium was chosen as the abisca value because it has the lowest detection limit and best precision. Osmium, Ir, Rh, and Re all show positive correlations (Figs. 4a–c). These elements are concentrated in pyrrhotite and pentlandite relative to cubanite and chalcopyrite (Figs. 4c; Tables 5, 6). Osmium and Ir values are almost identical at 0.2–4 ppm in both pyrrhotite and pentlandite. Cabri et al. (2003) reported similar to slightly lower values at 0.1–1.5 ppm. Chalcopyrite and cubanite contain 0.002–0.02 ppm Os and Ir. Cabri et al. (2003) reported that their values for Os and Ir in chalcopyrite were less than detection (approximately 0.005 ppm).

Rhenium values vary between 0.1 and 0.6 ppm in pyrrhotite and pentlandite and between 0.001 and 0.01 ppm in chalcopyrite and cubanite. There are no literature values with which these results can be compared. Rhodium values in pentlandite and pyrrhotite vary between 10 and 100 ppm. Cabri et al. (2003) and Czamankse et al (1992) report similar values. Rhodium contents in the chalcopyrite and cubanite are in the 0.1–2 ppm range. Neither, Cabri et al. (2003) nor Czamankse et al. (1992) obtained results for Rh in chalcopyrite or cubanite.

Ruthenium and Ir show positive correlation in pyrrhotite and pentlandite, with concentrations in the range 2–20 ppm for Ru (Fig. 4d). Cabri et al. (2002,

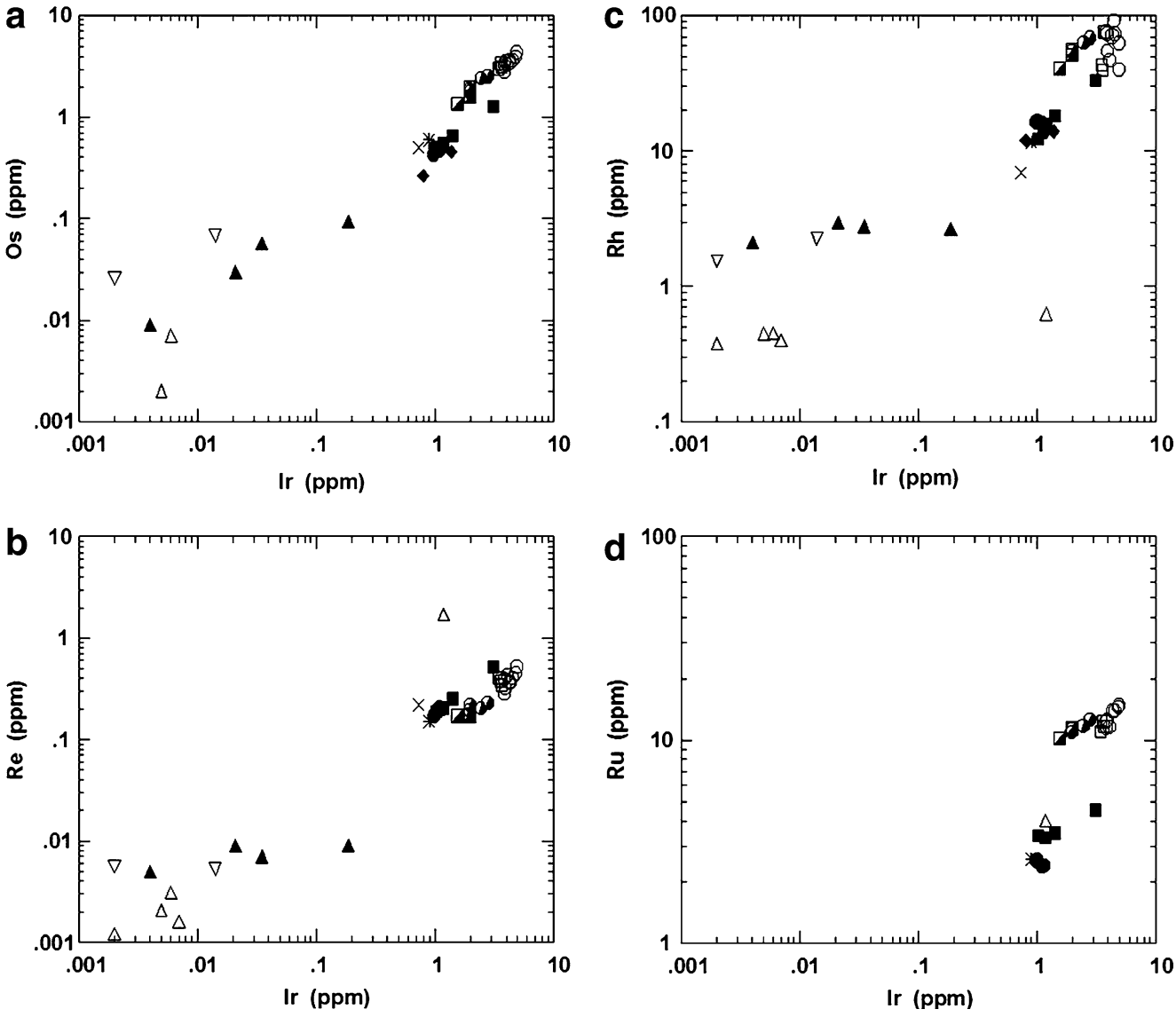

Fig. 4 Ir versus **a** Os, **b** Re, **c** Rh and **d** Ru. Note that the IPGE and Re show good correlation with each other indicating that they were concentrated by the same phase, probably MSS. The calculated sulfide liquid composition falls on the trend defined by the sulfide minerals indicating these elements are largely contained in these sulfides

2003) report similar values 0–11 ppm in pyrrhotite and pentlandite.

Discussion

Mass balance of the PGE and other chalcophile elements

In order to consider whether most of the metals are present in the major sulfide minerals (pentlandite, pyrrhotite, chalcopyrite and cubanite) the concentration of the metals in the whole rocks were recalculated to 100% sulfides by assuming that all the metals are present in the sulfides and that they consist of pentlandite, pyrrhotite and chalcopyrite (Table 8). These values are shown as * and X on Figs. 2, 3, 4. For some elements (Ag, Co, Pd, Os, Ir, Re, Rh, Ru) the metals recalculated to 100% sulfides plot on the sulfide mineral trends (Figs. 2c, 3, 4) indicating that these metals are largely present in the sulfides. In contrast, for some elements (Zn, Cd, Pt and Au) the 100% sulfide metal values plot above the sulfide mineral trend suggesting that some other phase or phases containing these elements are present in the rocks. Ilmenite was observed in these samples and Genkin et al. (1982) have identified sphalerite as being present in much of the Noril'sk ore. Possibly these two minerals account for the balance of the Zn and Cd.

Table 8 Calculation of metal content of the sulfides from whole rock concentrations

Sample	S (%)	Ni (%)	Cu (%)	Co (ppm)	Re (ppm)	Os (ppm)	Ir (ppm)	Ru (ppm)	Rh (ppm)	Pt (ppm)	Pd (ppm)	Au (ppm)	Ag (ppm)	Cd (ppm)	Zn (ppm)
Whole rock concentrations of metals and S															
E-1	2.38	0.51	0.81	170	0.0079	0.030	0.061	0.170	0.750	4.2	10.0	0.343	2	2	150
AB	1.34	0.39	0.59	140	0.0056	0.017	0.025	0.075	0.235	1.0	6.1	0.125	2	2	70
Recalculated to 100% sulphides allowing for 0.02% Ni, 70 ppm Co, 60 ppm Zn in the silicate fraction															
E-1	36.43	7.55	12.3	1531	0.121	0.459	0.934	2.60	11.48	64.3	153	5.25	31	31	1378
AB	34.92	9.64	15.1	1824	0.146	0.443	0.651	1.95	6.12	26.1	159	3.26	52	52	261
Massive sulfide from Medvezky Creek for comparison															
MC-16	36.35	8.48	12.1	1414		0.083	0.273	0.517	3.095	67.8	66.1	3.34	34.6	6	147

In the case of Pt and Au a backscatter image analysis of one of the droplets, AB-1, using the scanning electron microscope at the University of Laval, found seven small (< 1 μm) noble metal inclusions in the sulfides. These were too small to analyze but the energy dispersive spectra indicate that four are Pt–bismithide-telluride grains one is a Pt–Fe alloy and one a Pd–Au grain.

The distribution of the metals among sulfides has been calculated in detail. The weight fraction (F) of each sulfide phase present in the rock was estimated as follows. The Cu was assumed to be present in the chalcopyrite–cubanite intergrowth. The amount of the intergrowth was calculated by $(Cu_{wr})/(Cu_{iss})$, where Cu_{wr} = Cu concentration in the whole rock (Table 8), Cu_{iss} = average Cu concentrations in the chalcopyrite-cubanite intergrowths (Table 7). The amount of pentlandite was calculated by $(Ni_{wr}–0.02)/(Ni_{pn})$, where Ni_{wr} = Ni concentration in the whole rock (Table 8), Ni_{pn} = average Ni concentration in pentlandite (Table 7). The amount of pyrrhotite was estimated by calculating how much S was left after forming cubanite–chalcopyrite intergrowth and pentlandite and assigning it to pyrrhotite $(S_{wr}–S_{iss} \times F_{iss}–S_{pn} \times F_{pn})/Ss_{po}$.

The percentage of each element in each sulfide phase was calculated by

$$\left(\frac{F_a C_a^i}{C_{wr}}\right) \times 100,$$

where F_a = Weight fraction of phase a, C_a^i = Concentration of element i in phase a, C_{wr} = Concentration of element i the whole rock.

As has been found by earlier workers (Distler 1994; Cabri et al. 2002) pentlandite hosts almost all the Pd in the rocks, with pentlandite containing 100 and 101% of the whole rock values (Table 9). Pentlandite is also the principle sulfide host of Co accounting for 44% in sample E-1 and 26% of the Co in sample AB. But over half of the Co in these samples is not present in sulfides. Re, Os, Ir, Ru are hosted mainly by pentlandite and pyrrhotite (61–198%; Table 9). Given the various uncertainties in the calculation we consider that all of these elements are essentially present in the sulfides. Rhodium is also concentrated in pentlandite and pyrrhotite, and in sample E-1 the 91% of the Rh is in these sulfides (Table 9). However in sample AB, the percentage of Rh present is calculated to be up to 300% of the whole rock values. The reason for this is not understood.

Chalcopyrite is the main host of Ag, followed by pentlandite. Sulfides appear to be the main host for Ag in these rocks accounting for 65% of the Ag. In contrast, although Zn and Cd are concentrated in chalcopyrite, this still only accounts for 7–16% of these elements.

Only 1–25% of the Au and Pt present could be accounted for by the sulfides and these elements are not concentrated in one particular sulfide. As mentioned earlier small inclusions of Pt and Au minerals were found in the sulfides and possible these elements are located in the inclusions.

Monosulfide solid solution fractionation

Based on the experimental partition coefficients (Table. 1), empirical observations and assuming pyrrhotite and pentlandite represent the exsolution product of mss (e.g., Kullerud et al. 19691968, Sinyakova et al. 2005), the enrichment of the IPGE and Re and depletion of Pt, Au, Cu, Ag, Cd and Zn, in these two phases (Figs. 5 a–c) supports the mss fractionation model (Fig. 6a). Similarily, Cu, Ag, Cd, Zn, Pt, Pd and Au should be enriched in the fractionated liquid, thus one might iss to be enriched in these elements and thus the exsolution products cubanite and chalcopyrite should be enriched in these elements. The Cu, Ag, Cd and Zn are enriched in cubanite and chalcopyrite, but clearly the Pt, Pd and Au are not (Fig. 5d; Table 9).

Table 9 Weight percent of each element in each sulfide mineral and weight percent of the element in the sulfide fraction

Sample	Mineral	Ni (%)	Cu (%)	Co (%)	Re (%)	Os (%)	Ir (%)	Ru (%)	Rh (%)	Pt (%)	Pd (%)	Au (%)	Ag (%)	Cd (%)	Zn (%)
Sample E-1															
Percent of element in	cb/cp	8.30	99.38	4.18	2.5	4.2	2.7	ND	9.3	9.2	3.1	0.1	NA	8.4	19.6
Percent of element in	Pentlandite	85.50	0.67	43.15	40.9	28.6	30.3	30.1	31.0	4.1	101.5	0.0	NA	1.8	0.1
Percent of element in	Pyrrhotite	2.60	0.02	1.27	58.6	39.1	42.3	35.8	55.6	11.7	0.6	0.6	NA	2.0	0.1
Percent of element in	These sulfides	96.44	100.08	48.61	102.0	71.8	75.2	66.0	91.9	24.9	105.2	0.7	NA	12,3	19,8
Sample AB															
Percent of element in	cb/cp	6.05	99.36	1.70	1.4	2.1	0.5	ND	9.0	5.7	7,6	1.2	54.9	7.1	16.5
Percent of element in	Pentlandite	92.20	0.25	26.08	51.9	151.6	116.9	161.6	231.8	15.4	100.5	13.3	9.6	0.8	0.1
Percent of element in	Pyrrhotite	0.81	0.02	0.24	10.7	35.7	26.9	37.0	62.4	2.9	0.2	3.6	0.4	0.1	0.0
Percent of element in	These sulfides	99.06	99.64	28.02	64.0	189.3	144.3	198.6	303.2	24.0	108.3	18.1	64.9	8.1	16.6

This may be explained by the fact that experimental work shows that Pd and Pt do not partition into iss (Peregoedova 1998), by analogy we argue that Au does not partition into iss. Thus, the fractionated liquid becomes enriched in Ag, Cd, Cu, Zn, Pd, Pt and Au until iss crystallizes (Fig. 6b), at this point further fraction-

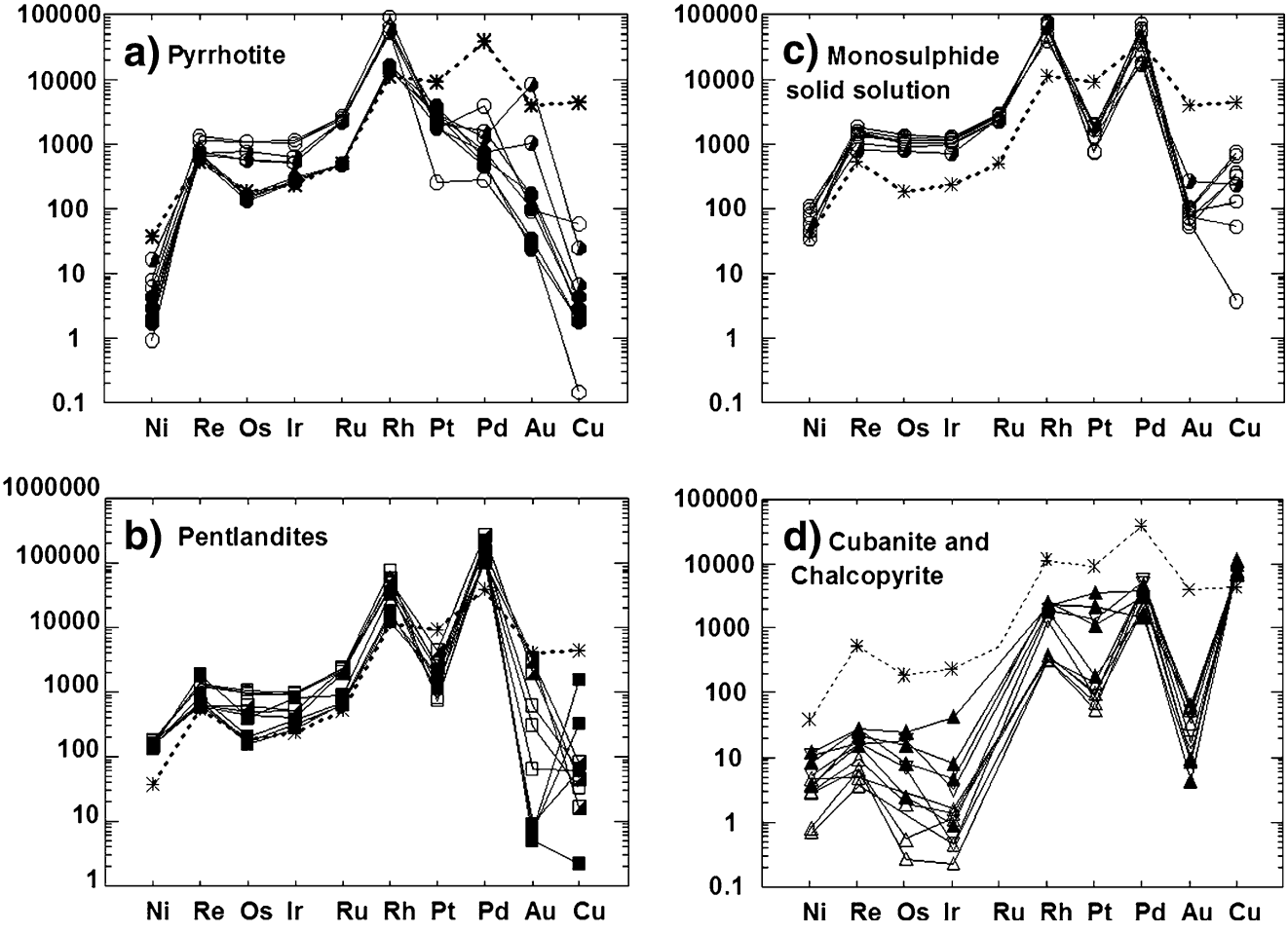

Fig. 5 Metal mantle normalized plots for; **a** pyrrhotite, **b** pentlandite, **c** mss and **d** cubanite–chalcopyrite. *Dashed lines* represent the calculated sulfide liquid composition. Relative to the liquid pyrrhotite is enriched in IPGE and Re and depleted in Pt, Pd, Au and Cu. This is consistent with MSS fractionation. Pentlandite shows similar enrichment and depletion, except for Pd, which is enriched in pentlandite. The mss has pattern that intermediate between pentlandite and pyrrhotite. The Cu-bearing phases are depleted in all the metals (except Cu) relative to the liquid. Mantle normalization factors from Barnes and Maier (1999)

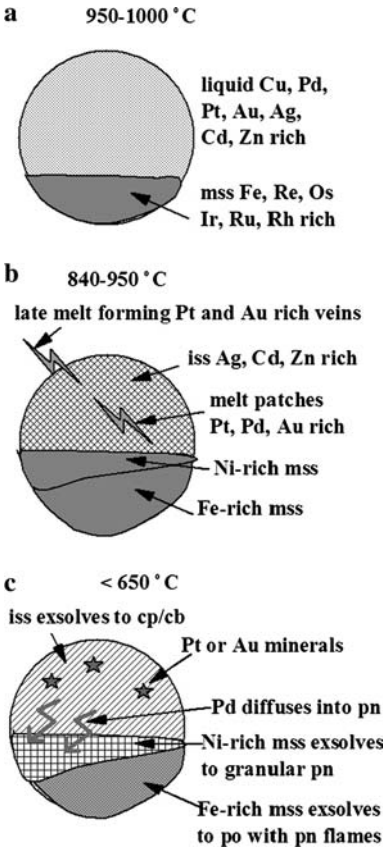

Fig. 6 Model of the formation of the zonation in the droplet; **a** crystallization of Fe-rich mss, enriched in IPGE, at the base of the droplet with the formation of Cu-rich liquid, enriched in Ag, Cd, Zn and Pd and Pt, at the top of the droplet; **b** crystallization of iss and Ni-rich mss from the fractionated liquid; **c** exsolution of po and pn from mss with diffusion of Pd into the pn, exsolution of cp and cb from iss

ation will not increase Cu concentrations (because the partition coefficient of Cu into iss is approximately 1). In contrast Pt, Pd and Au concentrations continue to increase as iss and mss crystallize. Possibly as suggested by Distler (1994) and Genkin et al. (1982) the Au and Pt crystallized from the very last liquid as discrete minerals among the iss grains (Fig. 6c). In addition, as suggested by Prichard et al. (2004) the very last liquid could be injected as veins around the droplet and the Pt and Au may be found there.

Two types of pentlandite are present, the small flames in pyrrhotite (Fig. 1c) and coarse granular pentlandite with pyrrhotite and cubanite exsolutions at the contact between the pyrrhotite and chalcopyrite–cubanite intergrowth (Fig. 1a). The flames are too small to analyze by LA-ICP-MS, although the Ni content of the pyrrhotite analyses suggests that a few flames were present in most pyrrhotite analyses. Despite the fact that granular pentlandite is thought to have formed by exsolution form mss it contains the bulk of the Pd in the rocks (Fig. 5b; Table 9). Given the low partition coefficient of Pd into mss the Pd content would be expected below, thus the high Pd content of granular pentlandite suggests that it is not simply the exsolution product of mss. Experimental work shows that pentlandite can form by exsolution from iss (e.g., Peregoedova and Ohnenstetter 2002, their Fig. 4b) thus it could be argued that the granular pentlandite exsolved from iss. To test this idea we determined the PGE content of large crystals of pentlandite found in a Cu-rich vein at Medvezky Creek (sample A-2). Presumably the chalcopyrite and pentlandite exsolved from iss. The pentlandite is extremely poor in IPGE and even richer in Pd than the pentlandite this consistent with the idea the pentlandite in the massive sulfide exsolved from iss, which crystallized from fractionated liquid. The difference in the IPGE and Pd content of the pentlandite from the droplets and IPGE and Pd content of the massive sulfide (Table 7) suggests that the pentlandite did not form by exsolution from iss.

The granular pentlandite is found at the contact between the chalcopyrite–cubanite intergrowth and the pyrrhotite and contains exsolutions of pyrrhotite and cubanite. Most of the mss analyses in Table 6 come from these areas. Possibly these areas represent Ni-rich mss that crystallized towards the end of mss crystallization. As the temperature dropped granular pentlandite and pyrrhotite exsolved from the Ni-rich mss (Fig. 6c). Possibly Pd diffused from both the mss and iss into the pentlandite during the exsolution of these phases.

Numerical modelling of the sulfide droplet is complicated by the presence of exsolutions. Nonetheless, we feel the results are worth considering. Assuming a Raleigh fractionation model the liquid composition i.e., the Cu-rich portion of the droplet could be modelled by

$$C_{\mathrm{L}} = C_{\mathrm{i}} F^{(D-1)}$$

Where C_{L} = Concentration of an element in the fractionated liquid, C_{i} = Concentration of an element in the initial liquid, F = weight fraction liquid remaining D = partition coefficient of an element into mss.

This equation may be rearranged to solve for D

$$D = \frac{\ln\left(C_{\mathrm{L}}/C_{\mathrm{i}}\right)}{\ln(F)+1}.$$

Assuming that the cubanite–chalcopyrite intergrowth represents the liquid fractionation then F = weight fraction of cubanite–chalcopyrite,

Table 10 Calculation of partition coefficients between monosulfide solid solution and sulfide liquid

	Co	Re	Os	Ir	Rh	Ag	Cd	Zn
	Calculated partition coefficents							
E-1	2.69	4.31	3.36	3.90	2.76		0.49	0.02
AB	6.43	9.04	10.61	13.11	8.30	0.38	0.29	0.02
	Calculated sulfide liquid $C_i = F_{iis} \times C_{iss} + F_{po} \times C_{po} + F_{pn} \times C_{pn}$ (ppm)							
E-1	1265	0.156	0.411	0.881	13.24		4.00	451
AB	976	0.096	0.870	0.975	19.44	33.29	4.17	299

C_L = concentration of the element in chalcopyrite–cubanite. Assuming that the system is closed C_i can be estimated by;

$$F_{iss} \times C_{iss} + F_{pn} \times C_{pn} + F_{po} \times C_{po}.$$

The calculated partition coefficients (Table 10) for Re, Os, Ir, Rh and Ag are similar to those found by experimental work (Table 1). There are no experimental values for Cd and Zn but our calculated values are consistent with the suggestion based on whole rock data that these elements do not partition into mss. As has been discussed above Au, Pt and Pd appear to have been redistributed during exsolution and thus partition coefficients for these elements were not calculated.

Conclusions

Palladium and Co are largely concentrated in pentlandite. Some of this pentlandite is as flame exsolutions in the pyrrhotite and thus efficient Pd extraction would require Pd to be extracted both from the granular and exsolution pentlandite. Platinum and Au are not concentrated in the sulfides and are probably present as discrete minerals. Osmium, Ir, Re and Rh are concentrated in the pyrrhotite and pentlandite. Silver, Cd and Zn are largely concentrated in the Cu-bearing phases.

The observed distribution of the PGE within the sulfides can be explained by assuming the lower part of the droplets formed by the crystallization of mss and the IPGE and Re were collected by the mss. The upper portion of the droplet formed by the crystallization of iss from the fractionated liquid and Cu, Ag, Cd and Zn partitioned into the iss. Gold and Pt were retained in the very last liquid and crystallized as discrete minerals among the iss grains. As temperature dropped pyrrhotite and pentlandite exsolved from the mss and chalcopyrite and cubanite exsolved from the iss. At some point Co and Pd diffused into the pentlandite, but the details of the mechanism for this is not clear to at this time.

Acknowledgments We would like to thank: Igor Migachev, Alexi Volchhov, Victor Ye Kunilov and Alexander P. Likhachev for arranging and facilitating a site visit to the Noril'sk-Talnakh area; Dr. Thomas Meisel for providing isotope dilution analyses of our sulfide standard, Dr. Paul Bedard for having the bright idea of installing a collision cell on our ICP-MS, the two reviews Drs. C. Ballhaus and H.Prichard. This work was financed by an NSERC Discovery Grant and Canadian Research Chair in Magmatic Metallogeny.

References

Ballhaus C, Tredoux M, Spath A (2001) Phase relations in the Fe–Ni–Cu–PGE–S system at magmatic temperature and application to the massive sulphide ores of the Sudbury igneous complex. J Petrol 42:1911–1926

Barnes S-J, Maier WD (1999) The fractionation of Ni, Cu and the noble metals in silicate and sulfide liquids. In: Keays RR, Lesher CM, Ligthfoot PC, Farrow CEG (eds) Dynamic processes in magmatic ore deposits and their application in mineral exploration. Geological Association Canada, Short Course 13:69–106

Barnes S-J, Acterberg E, Makovicky E, Li C (2001) Proton probe results for partitioning of platinum-group elements between monosulphide solid solution and sulphide liquid. S Afr J Geol 104:275–286

Brenan JM (2002) Re–Os fractionation in magmatic sulfide melt by monosulfide solid solution. Earth Planet Sci Lett 199:257–268

Bockrath C, Ballhaus C, Holzheid A (2004) Fractionation of the platinum-group elements during mantle melting. Science 305:1951–1953

Cabri LJ, Wilson JMD, Distler VV, Kingston D, Nejedly Z, Sluzheniken SF (2002) Mineralogical distribution of trace platinum-group elements in the disseminated sulphide ores of Noril'sk 1 layered intrusion. Trans Ins Min Metal Sect B Applied Earth Sci 111:B15–B22

Cabri LJ, Sylvestor PL, Tubrett MN, Peregoedova A, Laflamme JHG (2003) Comparison of LAM-ICP-MS and micro-PIXE results for Palladium and Rhodium in selected samples of Noril'sk and Talnakh sulfides. Can Mineral 41:321–329

Cox RA, Barnes SJ (2005) A method for in–situ analysis of trace-element variations in s using LA-HEX-ICP-MS. In: Tormanen TO, Alapieti TT (eds) 10th international platinum symposium, extended abstracts, Geological Survey of Finland, Espoo, pp 62–65

Czamanske GK, Kunilov VE, Zientek ML, Cabri LJ, Likhachev AP, Calk LC, Oscarson (1992) A proton-microprobe study of sulphide ores from the Noril'sk-Talnakh district Siberia. Can Mineral 30:249–287

Distler VV (1994) Platinum mineralization of the Noril'sk deposits. In: Lightfoot PC, Naldrett AJ (eds) Proceedings of Sudbury-Noril'sk symposium, Ont Geol Surv Spec 5:243–260

Fleet M, Chryssoulis SL, Stone WE, Weisener CG (1993) Partitioning of platinum-group elements and Au in the Fe–Ni–Cu–S system: experiments on the fractional crystallization of sulphide melt. Contrib Mineral Petrol 115:36–44

Gemoc (2006) Analytical methods. http://www.es.mq.edu.au/gemoc/

Genkin AD, Distler VV, Gladyshev GD, Filimonova AA, Evstigneeva TL, Kovalenker VA, Laputina IP, Smirnov AV, Grokhovskaya TL (1982) Copper-nickel sulphide ores of the Noril'sk deposits: Canada Centre for Mineral and Energy Technology, Mineral Research Program, Mineral Sciences Laboratory, Division Report MRP/MSL 82–90(LS), 220 p [Translated from the Russian, Sul'fidnye mendo-nikelevye rudy Noril'skikh mestorozhdenii, Akademika Nauk SSSR, Nauka, Moscow, 1981]

Griffin WL, Spetsius ZV, Pearson NJ, O'Reilly SY (2002) In situ Re-Os analysis of sulfide inclusions in kimberlitic olivine: New constraints on depletion events in the Siberian lithospheric mantle. Geochem Geophys Geosyst 3:1069

Jackson SE, Longerich HP, Dunning GR, Freyer B (1992) The application of laser-ablation microprobe; inductively coupled plasma-mass spectrometry (LAM-ICP-MS) to in situ trace-element determinations in minerals. Can Mineral 30:1049–1064

Kozyrev SM, Komarova MZ, Emelina LN, Oleshkevich OI, Yakovleva OA, Lyalinov D, Maximov VI (2002) The mineralogy and behaviour of the PGM during processing of the Noril'sk-Talnakh PGE-Cu-Ni ores. In: Cabri LJ (ed) The geology, geochemistry, mineralogy and mineral benification of platinum-group elements. Can Inst Min Metall Spec 54:757–792

Kullerud G, Yund RA, Moh GH (1969) Phase relations in the Cu–Fe–S, Cu–Ni–S and Fe–Ni–S systems. Econ Geol Monogr 4:323–343

Li C, Barnes S-J, Makovicky E, Rose-Hansen J, Makovicky M (1996) Partitioning of Ni, Cu, Ir, Rh, Pt and Pd between monosulfide solid solution and sulfide liquid: effects of composition and temperature. Geochim Cosmochim Acta 60:1231–1238

Lightfoot PC, Naldrett AJ, Hawkesworth CJ (1984) The geology and geochemistry of the Waterfall Gorge section of the Insizwa complex with particular reference to the origin of the nickel sulfide deposits. Econ Geol 79:1857–1879

Lorand JP, Alard O (2002) Platinum-group element abundances in the upper mantle: New constraints from in situ and whole-rock analyses of Massif Central xenoliths (France). Geochimi Cosmochim Acta 65:2789–2806

Mason PRD, Kraan WJ (2002) Attenuation of spectral interferences during laser ablation inductively coupled plasma mass spectrometery (LA-ICP-MS) using an rf only collision and reaction cell. J Atomic Absorp Spectrosc 17:858–867

Meisel T, Fellner N, Moser J (2003) A simple procedure for the determination of platinum group elements and rhenium (Ru, Rh, Pd, Re, Os, Ir and Pt) using ID-ICP-MS with an inexpensive on-line matrix separation in geological and environmental materials. J At Absorp Spectroscopy 18:720–726

Mackovicky E, Mackovicky M, Rose-Hansen J (1986) Experimental studies on the solubility and distribution of platinum-group elements in base metal sulphides in platinum deposits. In: Gallagher MJ, Neary C, Ixer RA, Prichard HM (eds) Metallogeny of basic and ultrabsic rocks. Inst Min Metall, London pp 415–425

Mackovicky E (2002) Ternary and quaternary phase systems with PGE. In The Geology, geochemistry, mineralogy and mineral benification of platinum-group elements. In: Cabri LJ (ed) The geology, geochemistry, mineralogy and mineral benification of platinum-group elements. Can Inst Min Metall Spec 54:131–175

Mungall JE, Andrews DRA, Cabri LJ, Sylvester PJ, Tubrett M (2005) Partitioning of Cu, Ni, Au, and platinum-group elements between monosulfide solid solution and sulfide melt under controlled oxygen and sulfur fugacities. Geochim Cosmochim Acta 69:4349–4360

Naldrett AJ, Asif M, Gorbachev NS, Kunilov VYe, Stekhin AI, Fedorenko VA, Lightfoot PC (1994) The composition of the Ni-Cu ores of the Oktyabr'sky deposit, Noril'sk region. In: Lightfoot PC, Naldrett AJ (eds) Proceedings of Sudbury-Noril'sk symposium, Ontario Geol Surv Spec 5:357–373

Peregoedova AV (1998) The experimental study of the Pt–Pd-partitioning between monosulfide solid solution and Cu–Ni–sulfide melt at 900–840°C. In: 8th international platinum symposium abstracts. Geol Soc South Africa and South African Inst. Min. Metall. Symposium Series S18:325–327

Peregoedova AV, Ohnenstetter M (2002) Collectors of Pt, Pd and Rh in a S-poor Fe–Ni–Cu–sulfide system at 760°C: experimental data and application to ore deposits. Can Mineral 40:527–561

Peregoedova AV, Barnes S-J, Baker DR (2004) The formation of Pt–Ir alloys and Cu–Pd rich sulfide melts by partial desulfurization of Fe–Ni–Cu sulfides: results of experiments and implications for natural systems. Chem Geol 208:247–264

Peregoedova AV, Barnes S-J, Baker D (2006) Formation of Ru–Os alloys and laurite $(RuOs)S_2$ in the presence of monosulfide solid solution and sulfide liquid in the system Fe–Ni–Cu–S. Can Min (in press)

Prichard HM, Hutchinson D, Fisher PC (2004) Petrology and crystallization history of multiphase sulfide droplets in a mafic dike from Uruguay. Econ Geol 99:365–376

Sinyakova EF, Kosyakov VI, Kolonin GR (2001) Behavior of PGE on the cross-section of melts in the system Fe-Ni-S (FexNi0.49-xS0.51). Russ J Geol Geophys 42:1287–1304

Sinyakova EF, Kosyakov VI, Nenashev B, Tsirkina NL (2005) Single-crystal growth of $Fe_yNi_{1-y}S_{1-d}$ solid solution. J Cryst Growth 275:e2055–e2060

Stekhin AI (1994) Mineralogical and geochemical characteristics of the Cu-Ni ores of the Oktyabr'sk and Talnakh deposits. In: Lightfoot PC, Naldrett AJ (eds) Proceedings of the Sudbury-Noril'sk Symposium: Ontario Geological Spec 5:217–230

Wallace P, Carmichael ISE (1992) Sulfur in basaltic magmas. Geochim Cosmochim Acta 56:1863–1874

Zientek ML, Likhachev AP, Kunilov VE, Barnes S-J, Meier AL, Carlson RR, Briggs PH, Fries TL, Adrian BM (1994) Cumulus processes and the composition of magmatic ore deposits: examples from the Talnakh district, Russia. In: Lightfoot PC, Naldrett AJ (eds) Proceedings of the Sudbury-Noril'sk Symposium. Ontario Geological Survey, Spec. 5:373–392